Status of the Sardinia Radio Telescope as a receiver of the BIRALET radar for space debris observations

Pisanu, Tonino, Schirru, Luca, Urru, Enrico, Maxia, Paolo

Tonino Pisanu, Luca Schirru, Enrico Urru, Paolo Maxia, "Status of the Sardinia Radio Telescope as a receiver of the BIRALET radar for space debris observations," Proc. SPIE 11445, Ground-based and Airborne Telescopes VIII, 114457B (13 December 2020); doi: 10.1117/12.2576249

SPIE.

Event: SPIE Astronomical Telescopes + Instrumentation, 2020, Online Only

Status of the Sardinia Radio Telescope as receiver of the BIRALET radar for space debris observations

Tonino Pisanu *[a], Luca Schirru[a], Enrico Urru[b], Paolo Maxia[a]
[a]National Institute for Astrophysics (INAF), Cagliari Astronomical Observatory, Via della Scienza 5, 09047 Selargius, Italy; [b]Italian Space Agency (ASI), Via Del Politecnico Snc, Rome, 00133, Italy.

*tonino.pisanu@inaf.it

ABSTRACT

Space debris are human-made objects, of variable sizes and shapes, that orbit the Earth or reenter the atmosphere. They represent a serious problem for every active spacecraft and satellite, due to the high risk of collision and consequently the generation of new debris. One of the main segments of the Space Situational Awareness program regards space surveillance and tracking activities, with procedures for tracking resident space objects, using a sensor network composed by radars, telescopes and lasers. In this way, it is possible to collect data in order to catalogue and perform orbit predictions of objects orbiting the Earth, with the aim of avoiding collisions between them. One of the Italian radars for space and surveillance tracking functions is represented by the BIRALET system, an acronym which stands for Bi-static Radar for LEO Tracking. This radar operates in P-band at 410-415 MHz, is a bi-static configuration composed of a transmitting 7-meter antenna and the SRT (Sardinia Radio Telescope) as receiver, with a baseline of about 20 km. The Sardinia Radio Telescope is a 64-meter fully steerable wheel-and-track antenna, located near San Basilio (Cagliari, Sardinia, Italy). It represents a flexible instrument used for radio astronomy and space science studies, developed to work in a wide frequency range between 300 MHz and 110 GHz. In this paper, we present a review of the status of the SRT for space debris observation. In particular, we describe three possible system configurations, in order to perform Doppler shift and range measurements. In particular, we present a simplified solution based on a spectrum analyzer as a back-end that permits only Doppler shift measurements. Another more complex solution for Doppler shift measurements, is based on the electronic Red Pitaya board. For the Red Pitaya we developed also a dedicated signal acquisition chain with a down-conversion circuit, in order to shift the received signal in the frequency range of the board. Finally, a more complex solution that allows range and range rate measurements, based on the National Instrument USRP board as a back-end. For future developments, we present the possibility to improve our system, using a C-band Phased Array Feed as a receiver.

Keywords: Sardinia Radio Telescope, BIRALET radar, P-band, space debris observations, Doppler shift, range and range rate measurements.

1. INTRODUCTION

Since 1957, rockets and satellites have been sent into space for several missions, during humanity's rapidly advancing space adventure . Most of these objects have lost their original activity over time, but are still orbiting out of control around the Earth or reentering the atmosphere as space debris[1]. They represent a serious problem for every active satellite or spacecraft, because collisions between in-orbit objects can occur from every direction with speeds up to 10 km/s and consequently they risk creating new debris, as explained by the Kessler syndrome[2]. Moreover, during the re-entering process, most debris burns up in the atmosphere, but larger debris can reach the ground intact. The most crowded orbit is the Low Earth Orbit (LEO), between 200 and 2000 km of altitude, where pieces of debris are denser than meteoroids[3].

An important space debris mitigation measure is represented by collision avoidance procedures. They require an accurate knowledge of the state of the orbiting objects, and consequently it is necessary to have a dedicated sensor network to collect useful data for orbit determination processes. Thanks to the Space Surveillance Network (SSN)[4], the United States Strategic Command (USSTRATCOM) is able to maintain the largest database of catalogued objects in LEO[5], with about 24000 trackable objects with sizes greater than 10 centimeters[3]. The United States Joint Space Operations Center

Ground-based and Airborne Telescopes VIII, edited by Heather K. Marshall, Jason Spyromilio, Tomonori Usuda, Proc. of SPIE Vol. 11445, 114457B · © 2020 SPIE
CCC code: 0277-786X/20/$21 · doi: 10.1117/12.2576249

(JSpOC), using data coming from the sensors network, performs orbit determination with its own software and elaborates the orbital parameters for making them available in a universally suitable format, i.e. the two-line element sets (TLEs)[6].

With the aim of aligning with the United States, the European Commission started, in 2015, a dedicated framework for European Space Surveillance and Tracking (EUSST) in the Space Situational Awareness program. Within this framework, a network of dedicated sensors (radars, telescopes and lasers) for the surveillance and tracking of resident and re-entering objects, has been implemented. Laser and optical telescopes are used for observations in the Medium Earth Orbit (MEO), between 2000 and 35786 km of altitude, and in the Geosynchronous Equatorial Orbit (GEO), above 36000 km. Whereas, radar sensors are useful for measurement campaigns in LEO.

By concentrating on radar sensors, the analysis shows that Europe can count on a large network of radar sensors with different features. The European Incoherent Scatter Scientific Association (EISCAT), for instance, is a VHF and UHF radar system, composed of three separate sites located in Norway (Svalbard), Finland and Sweden[7]. All the EISCAT transmitters are able to supply a maximum peak power in the range of the Megawatts, with a duty cycle of about 10-20%. Germany has at its disposal a powerful bi-static radar consisting of the FGAN Tracking and Imaging Radar (TIRA), located near Bonn, as a transmitter, and the Max-Planck-Institute Effelsberg Radio Telescope as a receiver[8]. In this configuration, the system can transmit 1-2 MW peak power pulses in L-Band, allowing the detection of objects with a size down to 1 cm. In the next future, the German Space Administration (DLR) will include the German Experimental Surveillance and Tracking Radar (GESTRA)[9] among the active radar sensors. GESTRA is a close-monostatic pulsed phased array working in L-band (1280-1400 MHz), able to perform digital beamforming. On the French side, remarkable radar facilities for SD are the Grand Réseau Adapté à la Veille Spatiale (GRAVES), a military continuous wave (CW) bi-static phased array VHF radar, operating at 143.05 MHz, located in Dijon[10] and the ARMOR, a mono-pulse C-band system with 1 MW peak power[11] located on the missile range instrumentation ship "Monge". Regarding Spain, the Spanish Space Surveillance and Tracking (S3T) system is currently equipped with two radars: the Monostatic Space Surveillance Radar (MSSR), a close-monostatic L-band radar, located in the Santorcaz military naval base, and the new S3T Surveillance Radar (S3TSR)[12]. In the United Kingdom, in 2010, the Chilbolton radar, a fully steerable 25-m dish antenna working in S-band (3 GHz) with a peak power of 700 kW, located near Winchester (Hampshire), was converted, for SST purposes, in the Chilbolton Advanced Satellite Tracking Radar (CASTR). These features allow the CASTR to efficiently detect objects with Radar Cross Section (RCS) greater than 0.5 squared-meters in LEO[13].

Italy is part of the EUSST project and, regarding radar sensors, two bi-static radars based on radio telescopes as receiver are made available for space debris survey and tracking observations. They are the BIRALES system[14], which acronym stands for Bi-static Radar for LEO Survey, and the BIRALET system[15], which acronym means Bi-static Radar for LEO Tracking. Both bi-static radars have same transmitter, named Radio Frequency Transmitter (TRF) that works in P-band at 410-415 MHz. The receiver of the BIRALES radar is the Northern Cross Radio Telescope, located in the Medicina Radio Astronomical Station, near Bologna, in Northern Italy. This system is used for monitoring the space environment in survey and tracking mode. The receiver exploits a multi-beam configuration that provides, an estimate of the angular track of the transiting object in the receiver field of view obtained from the analysis of the beam illumination sequence. Along with the angular information, the BIRALES radar also measures range and range rate, illumination time and power intensity obtained by the Signal-to-Noise Ratio (SNR), This innovative configuration allows the sensor to perform initial orbit determination[16].

Whereas, the receiver of the BIRALET radar is the Sardinia Radio Telescope (SRT), a 64-meter fully steerable wheel-and-track parabolic antenna, located near San Basilio (Cagliari, Sardinia, Italy). It represents a flexible instrument used for radio astronomy studies and space science, developed to work in a large frequency range between 300 MHz and 110 GHz[17]. In this paper, we present a review of the status of the BIRALET radar for space debris observation, focusing on the description of the front-end (section 2) and the back-end of the system (section 3). In particular, we describe three possible configurations of the system in order to perform Doppler shift and range measurements. We present a simplified solution based on a Spectrum Analyzer as a back-end that permits Doppler shift measurements (sub-section 3.1); another more complex solution, for Doppler shift measurements, is based on the electronic Red Pitaya board (sub-section 3.2); and finally the most complex solution, which allows range and range rate measurements, using the National Instrument USRP board as a back-end (sub-section 3.4). In addition, we present a set of preliminary results of space debris campaigns collected by the BIRALET radar using these three SRT configurations (section 4).

2. THE FRONT-END OF THE ITALIAN BIRALET RADAR

The Italian BIRALET system, which acronym stands for Bi-static Radar for LEO Tracking, is a bi-static radar employed for space surveillance awareness activities, focused on space debris detection and tracking. This bi-static radar is composed of the Radio Frequency Transmitter (TRF) as transmitter, described in the following sub-section 2.1, and the Sardinia Radio Telescope (SRT) as receiver, outlined in the sub-section 2.2. Since there is a baseline between the transmitting and receiving antennas of about 20 km, and one needs space objects detection at distances from hundreds to thousands of kilometers, the radar might be approximately considered as a mono-static radar. The main features of the BIRALET radar are summarized in Table 1.

Antenna name	TRF	SRT
Frequency range	410-415 MHz	410-418 MHz
Antenna gain @410 MHz	27.3 dBi	46.6 dBi
Half Power Beam Width (HPBW)	7.3 deg	0.8 deg
Azimuth speed	3 deg/sec	0.85 deg/sec
Elevation speed	3 deg/sec	0.5 deg/sec
Polarization	Circular	Circular and linear
Side-lobes	<-20 dB	<-20 dB
Noise Temperature	NA	20 K

Table 1: Main features of the BIRALET radar.

2.1 The Radio Frequency Transmitter antenna

TRF is a fully steerable parabolic antenna with a 7-meter diameter dish (see Figure 1a), with a primary focus configuration, located in the Italian Joint Test Range in the region of "Salto di Quirra" (Lat. 39.6050°N – Log. 9.4396°E, Cagliari, Sardinia, Italy)[15]. The antenna has been manufactured to operate in a large frequency range up to 10 GHz with a high antenna efficiency. And in spite of the currently operative frequency of 410-415 MHz, this aspect is very attractive for future system upgrades to higher frequencies observations. Regarding the microwave components chain, the TRF system is made up of a set of seven power amplifiers able to transmit a root-mean-square power between 1 and 10 kW. The TRF amplification block is designed to work in the bandwidth of 402-420 MHz and filtered using a tunable central frequency (i.e. 410 MHz) with bandwidth of 5 MHz[15]. At this frequency, the system has a half power beam width (HPBW) of about 7 degrees and an antenna gain of about 27 dBi.

An important feature of the system is represented by its mechanical pointing speed, equal to 3 degrees per second in both azimuth and elevation directions, that permits to move the antenna very fast, between one observation target and another and, in other scenarios, to operate in tracking mode.

A simplified block diagram of the transmitting system, which includes a central control unit (CCU), an automatic gain control (AGC), a radio frequency splitter, a phase adjustable block and seven amplifier blocks, is given in Figure 1b. In detail, the CCU, which takes in an input signal, is linked to the AGC for the system gain adjustment. The AGC then sends the signal to the radio frequency splitter that creates seven signals, adjusted in phase, for all power amplifier. After the amplification block, the signals are combined, filtered and sent to the antenna.

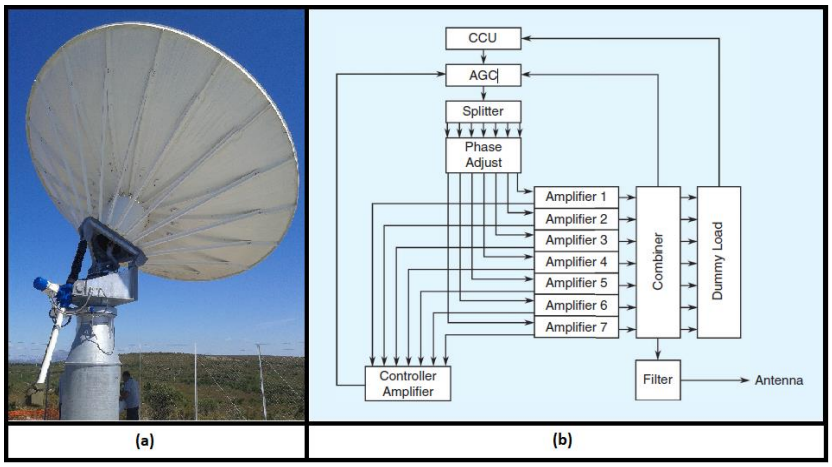

Figure 1.(a) the Radio Frequency Transmitter (TRF) antenna; (b) the block diagram of the transmitting system.

2.2 The Sardinia Radio Telescope

The receiver system of the BIRALET radar is the SRT antenna, located close to a Sardinian town named San Basilio (Lat. 39.493072°N - Long. 9.245151°E, Cagliari, Sardinia, Italy)[18]. SRT is a versatile instrument, designed for radio astronomy, geodynamical and space science studies, which is also utilized from 2014[17]for space situational awareness applications. The antenna is a multi-reflector system with a quasi-Gregorian configuration, composed of a quasi-parabolic 64-meters primary mirror and a 7.9-meter elliptical secondary mirror. SRT is equipped with three other mirrors (two with a diameter of 2.9 m and one with a diameter of 3.9 m), which form the Beam Wave-Guide (BWG) system. The telescope is able to host up to 20 remotely controllable receivers and to observe the sky with high efficiency in the frequency range between 0.3–116 GHz[18]. Equipped with an active surface system, SRT is one of the largest radio telescopes in the world that provides this technology[19]. A total of 1,116 electromechanical actuators can control the 1,008 aluminum panels of the primary mirror, which is supported by a stainless-steel trusses rear frame. The actuators help to compensate for possible undesired deformations of the primary mirror surface due to gravity, wind pressure, and thermal gradients[15].

Regarding the performances of the telescope for space debris applications, one important aspect concerns the azimuth and elevation mechanical maximum speeds, which are 0.85 and 0.5 degrees per second, respectively. Since, as we explained above, the transmitter works in P-band at 410-415 MHz, SRT has an antenna gain of about 46 dBi and a HPBW of about 0.8 degrees at this frequency range. These features allow observing of most space objects orbiting in LEO, that have a typical angular speed of <0.1 degrees per second, also in tracking mode[2].

The front-end employed for space debris radar campaigns is the dual-feed L-P receiver (see Figure 2), a cryogenically cooled (typically less than 20 K) coaxial receiver with two channels, one for the P-band (with a receiver frequency response at 410–418 MHz) and the other one for the L-band (at 1300–1800 MHz). This receiver is installed in the primary focus of the telescope[15] and it is composed by five main sections: the coaxial feed, the cryogenic front-end, the linear to circular polarizer, the noise calibrator and antenna unit injection, and the filter selector (see Figure 3a)[15]. The coaxial feed receives the Radio Frequency (RF) echo radar and sends it to the cryogenic front end, directly connected with the antenna unit injection and noise calibration, which perform the calibration of the whole system. Afterward, the RF signal is sent to the polarizer, which allows the system to keep the linear polarizations or to transform it in a circular polarization. The last stage allows the selection of a suitable filter, depending on the type of application. In particular, for space debris monitoring, a band pass filter (BPF) has been recently installed in the filter selector block (see Figure 3b). In particular, this BPF is a tubular filter (model 3B110-410/T15-O/O from K&L) centered at 410 MHz with a bandwidth of 402–418 MHz and an insertion loss of 1.1 dB. From the S_{21} red curve of Figure 3c, it is possible to appreciate the contribution of the space debris dedicated BPF, that confines the signal in the 3-dB bandwidth 402-418 MHz. The S_{21} red curve shows a maximum gain of about 27 dB, which matches, apart from some losses attributed to the coaxial cables used during the measurement, with the overall gain of the P-band receiver[15].

This filter guarantees a first discrimination of the frequencies of interest, reducing considerably the entire bandwidth of the P-band receiver, that originally is of 410-418 MHz[17]. The P-band receiver block is the first part of the acquisition chain, developed in order to utilize all the available back-ends, which are reported in Figure 4, 5 and 6.

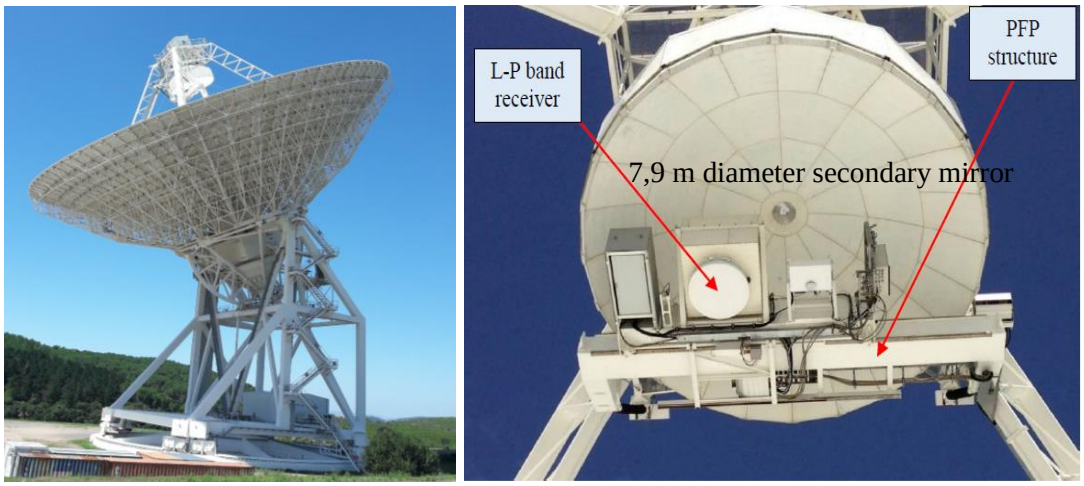

Figure 2. The Sardinia Radio Telescope (SRT) with its L-P receiver installed in the primary focus of the telescope.

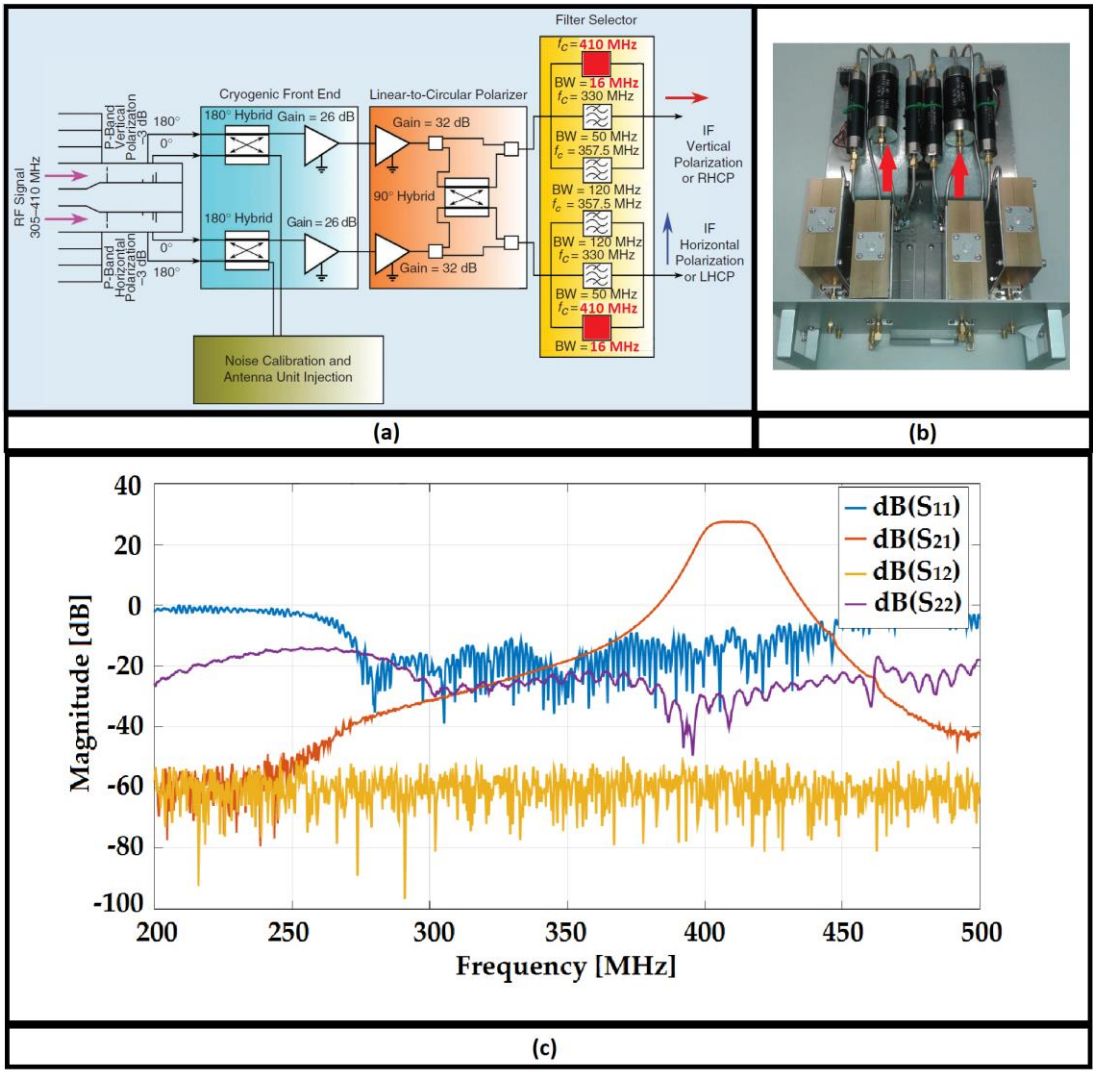

Figure 3. (a) schematic of the P-band receiver with the space debris BPFs highlighted in red; (b) A photo of the 16-MHz BW BPFs at 410 MHz (indicated by red arrows) mounted inside the filter selector block; (c) S-parameter of the P-band receiver.

3. THE ACQUISITION CHAINS AND THE BACK-ENDS OF THE ITALIAN BIRALET RADAR

Since 2014, SRT is employed in space situational awareness activities and consequently is equipped with a dedicated channel for space debris observations. This channel might have three main configurations depending on the utilized back-end. In fact, three back-ends based respectively on spectrum analyzer (sub-section 3.1), Red Pitaya board (sub-section 3.2) and National Instrument USRP 2954 board (sub-section 3.3), respectively, are available. Each configuration needs of a dedicated acquisition chain in order to carry the RF signal from the SRT feed to the back-end. As is the case for all acquisition chains, after the P-band receiver block, the RF signal enters the focus selector block (see Figure 4, 5 and 6), which permits the choice of the antenna focus for the observation (the primary focus in the case of space debris observations) and provides an overall gain of about 20 dB. From the top of the primary mirror, the echo radar signal is then carried down to a shielded room at ground level, by means of a 500-m optical link[15]. In the following sections, the three dedicated back-ends, with their acquisition chain, are described in detail.

3.1 The acquisition chain for the back-end based on Spectrum Analyzer for Doppler shift measurements

The simplest channel, for space debris application, of the SRT antenna includes a Spectrum Analyzer as a back-end, as shown in Figure 4. In particular, the two channels of the P-band receiver, one for each polarization (i.e. the two linear or circular polarizations), after the Focus Selector block and the 500-m optical link described above, are combined using a Power Combiner (ZFSC-2-2500-S+ model from Mini-Circuits). After the Power Combiner, the RF signal is displayed and recorded by the Spectrum Analyzer (FSV model from Rohde and Schwarz[20]). This measurement setup was used during the first space debris experiments with the SRT in April 2014[17]. In this way, it is possible to see in real time the echo radar with a resolution bandwidth less than 10 Hz (according to the Spectrum Analyzer specifics), but data processing could be poor, mainly due to the limitations of the spectrum analyzer, i.e. the slow frequency sweeps for low resolution bandwidths, thus preventing all data saving in real time.
This receiver chain is useful for maintenance and testing operations, where it is necessary to view immediately the received signal (i.e. echo radar) in the instrument display, without a post-processing elaboration.
Thanks to the configuration with the spectrum analyzer as back-end, SRT performs Doppler shift measurements with an expected accuracy equal to or less than 20 Hz.

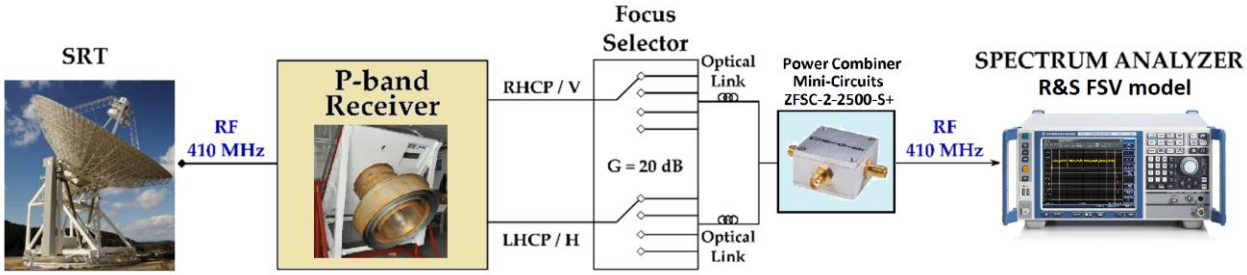

Figure 4. Receiver chain for the Spectrum Analyzer (FSV model from R&S) as backend.

3.2 The acquisition chain for the back-end based on Red Pitaya board for Doppler shift measurements

The second receiving chain was designed and realized with a dedicated back-end based on a Red Pitaya board, that permits the reduction of the global observation BW, limit the RF-interferences (RFIs) problem.. (see Figure 5).
The Red Pitaya board is a commercial System-on-a-Chip FPGA board provided with a dual-core 800 MHz ARM9 processor, an FPGA with 28000 logic cells, 512 MB of DDR3 RAM system memory, 2 RF inputs and 2 RF outputs, a sample rate of 125 MSample/s, a 14 bit Analog-to-Digital Converter (ADC) and a working frequency in the range 0-50 MHz[21]. For this reason, a down-conversion block, based on an appropriate frequency mixer (ZFM-2000 model from Mini-Circuits) was necessary, which allows the system to shift the RF signal from the 410 MHz to an Intermediate Frequency of 30 MHz. This signal is later filtered with a BPF (3LB30-30/T5-O/O model from K&L) centered at 30 MHz

with 5 MHz bandwidth and 0.9 dB of insertion loss[15]. After the filtering stage, a digital step attenuator (ZX76-31R75PP-S model from Mini-Circuits), controlled by the Red Pitaya, is inserted before the final amplifier (ZKL-1R5 model from Mini-Circuits) in order to avoid the saturation of the system.
A digital signal processing chain was programmed inside the Red Pitaya board[21], allowing the conversion of the analog input signal in a base-band complex raw signal. This raw signal can be stored and post-processed using a Fast Fourier Transform (FFT) and, finally, displayed in various plots such as spectrogram on the total acquisition time, data acquisition at the exact epoch of the debris passage and the time duration inside the beam of SRT.

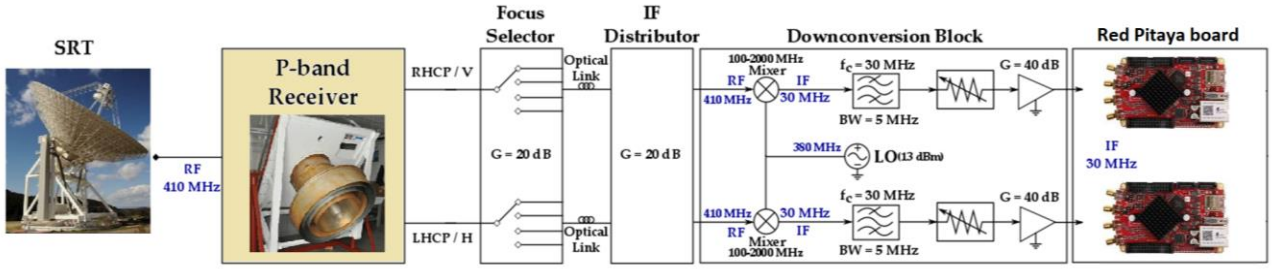

Figure 5. Receiver chain for the Red Pitaya board as backend.

Each Red Pitaya performs a digital down-conversion (DDC), which converts a real-time domain signal into a complex one centered in the baseband. The process of frequency conversion is achieved by mixing the input signal with a digital tone (i.e., a sinusoid) at 30 MHz. This creates two copies of the signal: one centered near zero and one centered at twice the tone frequency. This is possible using a second sinusoid out of phase by 90°. A direct digital synthesizer (DDS) generates the sinusoids internally. Once the baseband complex data is derived, low-pass filtering is necessary to remove an unwanted spectral information and avoid aliasing phenomena. Because a considerable decimation is needed, we used the well-known cascade-integrator comb finite-impulse response (CIC-FIR) chain. The CIC filter has proven to be an effective element in high-decimation systems; however, CIC filters present an unsatisfactory frequency response, thus, a FIR filter is used in cascade so as to compensate for the CIC response and, as a consequence, improve the overall filter response. The procedure creates a baseband complex signal that can be stored and subsequently divided into several sub-bands by means of a fast Fourier transform (FFT). The FFT engine could be implemented in the FPGA as well; however, the number of spectral points would be limited by the available memory on the FPGA. As a result, the engine was implemented in the CPU/GPU boards[15].
Finally, after Red Pitaya processing, by analyzing various produced plots, it is possible to extrapolate the Doppler shift measurement, with a resolution bandwidth less than 20 Hz, and the received SNR level[22].

3.3 The dedicated backend based on National Instrument USRP 2954 board for range and range rate measurements

On the wave of good results obtained using the back-ends described in sub-section 3.1 and 3.2, which permit only Doppler shift measurements, a new space debris dedicated back-end was developed in order to make also range measurements. In fact, as concerns orbit determination processes, the importance of the availability of possible range measurements, with the combined use of Doppler and range measurement, would grant both an increase in the object state estimate accuracy and a reduction in the estimated uncertainty.
The new back-end of the BIRALET system, funded and developed under the 2-32016-17 European Space Surveillance and Tracking Grant program, is based on a National Instrument USRP-2954 board[23]. The acquisition chain for this back-end is similar to that of the Spectrum Analyzer (sub-section 3.1). So here too, the two polarizations of the P-band receiver are combined using a Power Combiner (ZFSC-2-2500-S+ model from Mini-Circuits) and subsequently the combined signal at 410-415 MHz is processed by the USRP (see Figure 6).

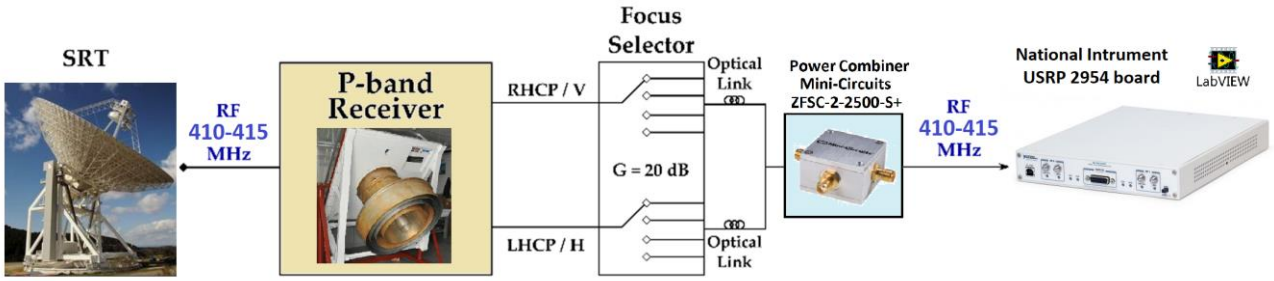

Figure 6. Receiver chain for the National Instrument USRP 2954 board as backend.

The same USRP board is also installed on the TRF, in order to transmit a well-known synthesized waveform signal that permits range and range rate measurement, simultaneously. In particular, the USRP board of the TRF antenna is configured to transmit a mixed signal composed of a chirp plus a continuous wave tone, which permit range and Doppler shift measurements.

In detail, the USRP-2954 board is used to generate the I/Q samples of the transmitted waveform. The I/Q samples are then converted into an analogue signal by two 16-bit DACs and up-converted by the I/Q up-converter chip[24]. Finally, this signal is amplified thanks to the 10 kW power amplifier of the TRF and it is transmitted towards the expected target position (predicted using the TLE[6]). The transmitter architecture is shown in Figure 7a.

The UHF signal at 410-415 MHz, received by SRT, is directly processed by the USRP-2954 board. This signal is then down converted to the board baseband by an I/Q down converter chip and finally digitalized by two ADCs. I/Q signals are then sent to the operator workstation for processing. The processing can be done both in real-time mode or in offline mode, by using the real time stored I/Q samples. This feature is extremely useful for testing purposes and for analyzing further improvements of the radar processing chain. The receiver architecture is shown in Figure 7b[24].

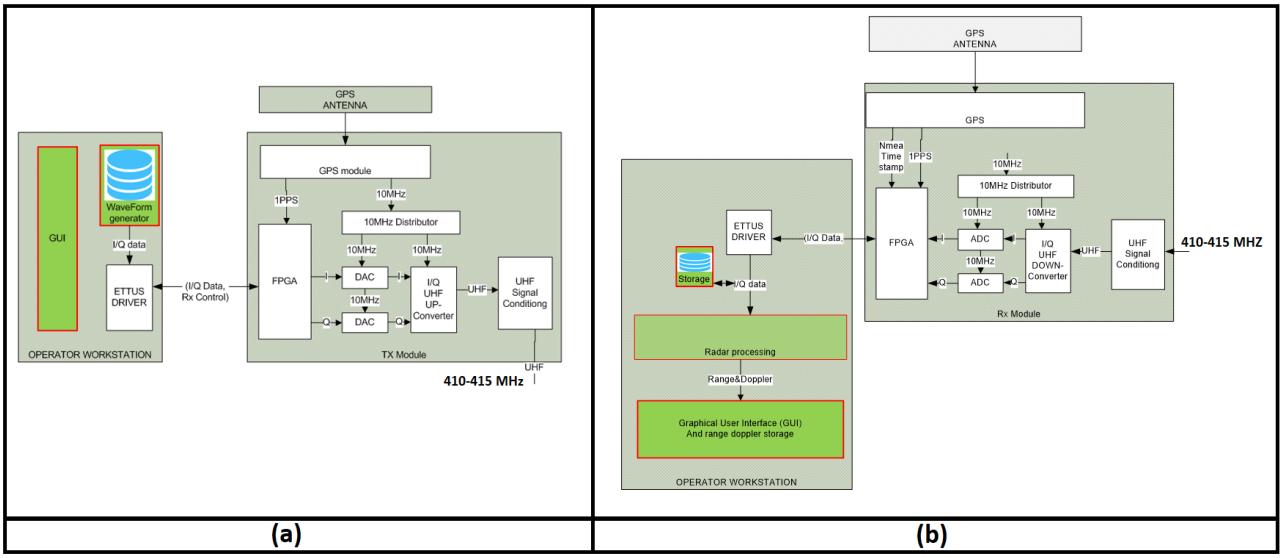

Figure 7. (a) transmitter architecture of the TRF antenna based on the USRP-2954 board; (b) receiver architecture of the SRT dedicated back-end based on the USRP-2954 board.

The overall performances of the radar are also determined by the TRF and SRT synchronization accuracy. The receiver and the transmitter are synchronized in time and frequency using the GPS 1PPS (pulse per second) and the 10 MHz reference signals. In particular, the 10 MHz signal is used as reference for all down-conversions and sampling frequency generation (ensuring no drift between transmitter and receiver); the 1 PPS signal is used to simultaneously start the acquisition/generation between receiver/transmitter. An integrated GPS receiver, installed in the USRP 2954 board, guarantees a maximum error of 10^{-7} seconds, that means 30 meters in distance.

The system has the ability to detect debris at a maximum range of 3000 kilometers with an accuracy of about 30 meters (as explained in the previous lines) and to perform also Doppler shift measurements with an accuracy of few Hertz. For this reason, the waveform transmitted by the TRF is a mixed signal composed of a frequency modulation continuous wave (FMCW) signal, better known as chirp, plus a continuous wave (CW) tone, with an overall bandwidth of 5 MHz, as shown in Figure 8.

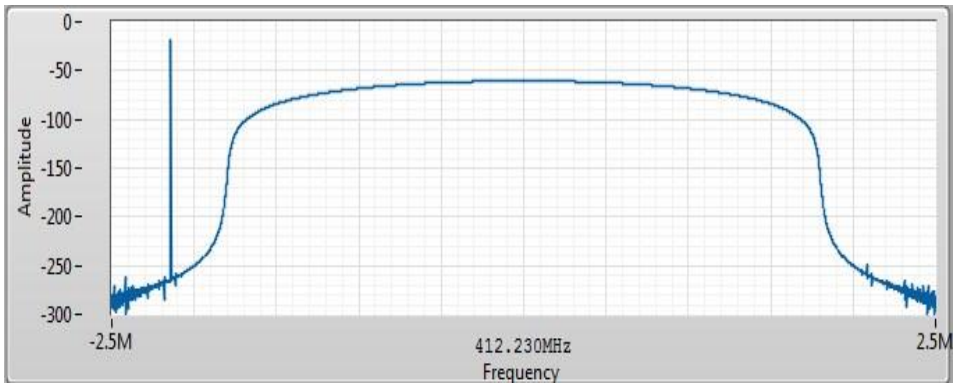

Figure 8. Transmitted signal composed of FMCW chirp plus a CW tone.

In particular, the transmitted signal is set to a central frequency of 412.23MHz, with the CW tone generated with an offset frequency of -2.145 MHz from the central one. Regarding the chirp, it is a down-chirp in the range of 3.6 MHz, a pulse repetition interval (PRI) of 20 ms and a pulse repetition frequency (PRF) of 50 Hz. This guarantees a range measurement of objects at distances up to 3000 km, as shown by the following formula[24]:

$$\mathrm{PRF} = \frac{c}{2d} \approx 50 \text{ Hz} \tag{1}$$

where c is the speed of light and d is the maximum range, in this case equal to 3000 km. This value of PRF prevents the possibility of Doppler measurements using only a pulsed signal, because typical space debris Doppler shift values in LEO are in the range of a few kilohertz (in P-band), values greater than our PRF. For this reason, the system transmits a chirp plus a CW tone, in order to work as a pulsed radar (for range measurements) and as a CW radar (for Doppler measurements).

The sampling frequency is 5 MS/s and the maximum RMS transmitting power is 10 KW, with a 100% duty cycle[24]. Using a 100% duty cycle allows us to use all the energy from the transmitter (there is no coupling between transmitter and receiver) and the 50 Hz PRF allows us to measure the range without ambiguities (the Doppler information, to compensate the range error, is extracted from the tone). Using a chirp of 3.6 MHz allows us to exploit all the usable bandwidth, maximizing the range resolution and leaving a small portion of the spectrum for the tone used for Doppler extraction. This permits a Doppler shift of more than 100kHz, more than sufficient, considering the expected target speed with the used carrier[24].

In order to maximize the signal to noise ratio for the range extraction, we used a matched filter to perform a pulse compression. The inter-pulse integration is also used by the addition of four chirps (see Figure 9). This aspect means that we have a measurement of the target range and Doppler, every 80 milliseconds (the step between each measure is four pulses: 20 ms * 4= 80 ms). Finally, both range and Doppler shift measurements are time stamped with a millisecond accuracy, allowing precise target trajectory prediction.

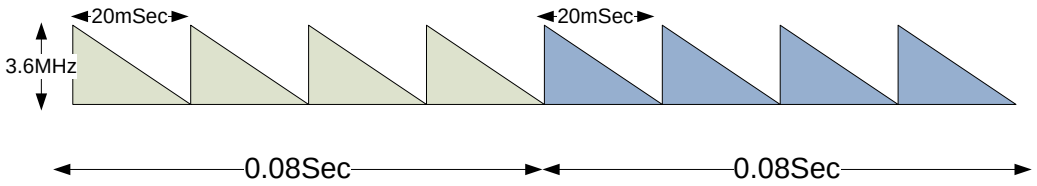

Figure 9. FMCW pulse train.

4. RESULTS OF SPACE DEBRIS OBSERVATIONS WITH THE ITALIAN BIRALET RADAR

In recent years, several measurement campaigns are performed. Between December 13th, 2018 and October 8nd, 2019, the BIRALET system was able to observe a total of 33 objects, using the dedicated back-ends based on the Spectrum Analyzer (sub-section 3.1) and the Red Pitaya board (sub-section 3.2). All the observations were made in beam-parking mode, waiting for the objects to cross the Field of View (FOV) of the antenna. The list of the scheduled passages for the debris, complete with the pointing coordinates, estimated radar cross section (RCS), estimated slant range (SR) and detection time for each object, is reported in Table 2. Before the observations, a forecasting campaign was made in order to obtain the azimuth and elevation pointing coordinates and to predict the Doppler shift frequency. An algorithm based on the reading of the TLEs provides these pieces of information. The predicted and the measured Doppler shift for each considered object is reported in Table 3.

NORAD ID OBJECT	AZIMUTH [DEG]	ELEVATION [DEG]	RCS [M2]	SR [KM]	DATE [MM/DD/YYYY]	TIME OF DETECTION [UTC]
6350	16.437	32.751	1.73	1694.078	12/13/2018	13:28:25
1328	79.358	75.448	2.16	1901.43	12/13/2018	13:48:19
26222	43.996	65.927	4.99	1571.70	12/13/2018	14:30:57
25482	33.651	62.505	1.06	1732.62	12/13/2018	15:00:36
30774	18.163	32.133	3.64	1526.68	12/13/2018	15:57:26
4256	87.967	75.484	0.51	1883.31	03/19/2019	14:36:20
39194	45.917	56.256	7.77	1068.92	03/22/2019	15:45:54
12150	49.961	72.920	5.07	2077.30	03/22/2019	16:07:03
28931	40.097	63.139	13.4	1540.01	03/22/2019	16:28:14
11166	126.647	70.556	6.05	1808.33	03/22/2019	16:53:39
7337	204.068	69.955	2.98	1952.61	09/06/2019	13:25:49
7646	311.755	50.602	0.17	2447.17	09/06/2019	14:38:30
36508	340.408	55.379	2.95	1700.43	09/06/2019	15:10:44
1328	94.379	66.816	2.16	2090.32	09/06/2019	15:43:55
39452	42.087	51.607	2.34	1080.77	09/06/2019	15:57:17
1328	118.746	72.537	2.16	1929.63	09/16/2019	12:08:18
42969	36.109	72.375	unknown	1727.42	09/16/2019	12:16:11
27944	60.085	53.297	0.13	1646.96	09/16/2019	13:31:07
1328	68.865	53.699	2.16	2220.55	09/16/2019	14:02:58
22824	99.517	53.116	0.16	1953.58	09/16/2019	14:45:45
36508	263.826	46.492	2.95	1918.60	09/16/2019	14:59:43
39453	321.540	48.670	2.41	1136.08	09/16/2019	15:29:59
15494	193.782	68.242	7.12	1071.12	10/08/2019	07:02:44

26102	22.286	60.228	3.35	917.86	10/08/2019	07:28:36
36119	58.139	63.318	2.18	1057.37	10/08/2019	07:34:44
3047	180.116	65.685	2.96	1557.96	10/08/2019	07:57:54
43243	182.686	79.956	unknown	586.60	10/08/2019	08:34:46
8458	253.576	71.252	2.02	1650.39	10/08/2019	08:48:32
40961	328.387	39.208	2.32	1955.37	10/08/2019	10:21:38
7363	18.799	67.056	4.76	1908.75	10/08/2019	11:36:22
33492	27.231	61.772	4.8	1500.13	10/08/2019	12:44:46
15595	44.335	63.236	9.3	1694.26	10/08/2019	14:10:37
25105	318.231	51.425	4.14	1876.84	10/08/2019	14:42:20

Table 2: Scheduled passages of the debris between December 13, 2018 and October 8, 2019.

NORAD ID object	**SNR [dB]**	**Estimated Doppler [kHz]**	**MEASURED Doppler [kHz]**	**Doppler error (Hz)**
6350	20.3	2.660	2.070	590
1328	22.9	-4.036	-3.300	-736
26222	32.2	-3.635	-3.486	-149
25482	7.5	-6.313	-6.480	167
30774	29.5	-1.590	-2.110	520
4256	24.6	-1.699	-1.650	-49
39194	12	4.222	4.440	-218
12150	20	-1.182	-0.872	-310
28931	34	-5.854	-4.660	-1.194
11166	17.5	-5.015	-4.280	-735
7337	18.5	4.872	4.900	-28
7646	25.3	4.641	5.360	-719
36508	31.3	9.215	9.600	-385
1328	10.7	-6.246	-6.380	134
39452	16.4	-8.657	-8.820	163
1328	25.7	-3.086	-3.120	34
42969	34.8	-3.290	-3.260	-30
27944	14.3	7.121	6.880	241
1328	16.4	-9.319	-9.416	97
22824	16.7	5.254	5.540	-286
36508	22.4	-3.731	-3.260	-471
39453	20.8	-9427	-9.750	323

15494	31.1	7.279	7.260	19
26102	17.1	-7.962	-7.440	-522
36119	23.5	5.778	5.620	158
3047	20.2	-7.192	-7.280	88
43243	16.5	-4.042	-4.240	198
8458	32.0	3.543	3.400	143
40961	18.1	9.587	9.922	-335
7363	19.5	-6.636	-6.660	24
33492	19.9	8.486	8.160	326
15595	16.2	7.799	7.420	379
25105	21.7	-7.693	-8.040	347

Table 3: Estimated and measured Doppler shift for the detected debris between December 13, 2018 and October 8, 2019.

For clarity, the spectrogram of the entire observation window for the objects with NORAD ID 4256, as well as the passage inside the beam of the SRT for each debris in the list, are shown in Figure 10. As it can be seen from the analysis of the results in Table 3, every debris in the list was correctly detected. Due to the relative close proximity of the transmitter with the SRT, the radio telescope was able to receive the carrier frequency (410.085 MHz), which is clearly visible in the images (Figure 10a). Additionally, in the spectrogram (Figure 10a), it is recognizable the frequency swipe of the debris echo, due to its high velocity, as it moves toward the receiver position (when the echo is located to the left of the carrier, which implies a negative Doppler shift) or as it moves away from it (when the echo is located to the right of the carrier, which implies a positive Doppler shift). The passage inside the beam of the SRT is a representation of the portion of the beam's footprint covered by each debris during its passage. This particular subject is a case in study that might be worth to be further investigate. At this stage, we may assume that the diameter of this footprint is ideally equal to the width of the HPBW (0.8 degrees). As it can be seen from the figures, the distance travelled inside the SRT beam, for every debris listed, is smaller than this value. The degrees travelled for each debris are evaluated taking into account the transit time and the angular velocity (which was calculated from the Doppler frequency and reported in Table 2). The likely implication is that the debris does not pass through the beam's center, but instead in a peripheral area. This drawback is easily explainable with a very small inaccuracy in the estimation of the pointing coordinates.

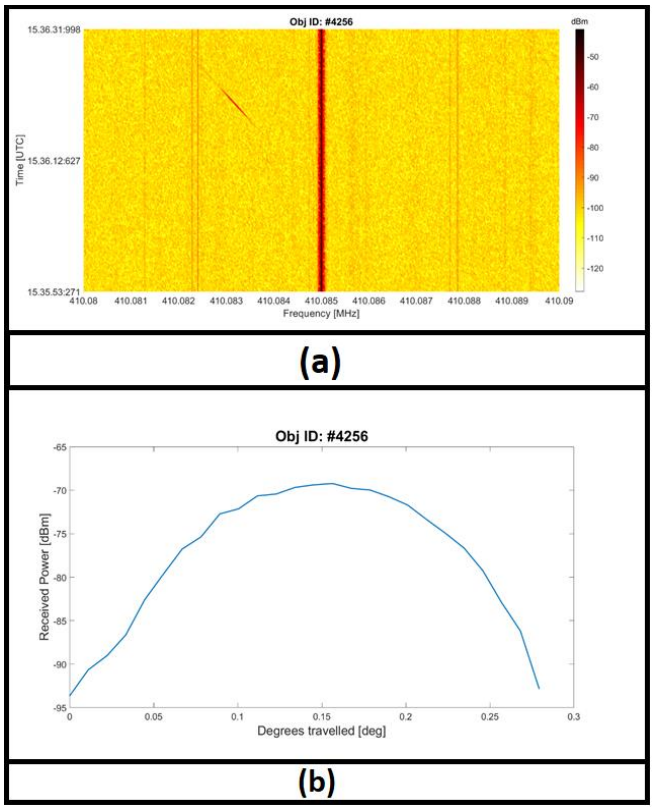

Figure 10. Debris NORAD ID 4256: (a) spectrogram; (b) passage inside the beam of the SRT.

In addition, a validation campaign of the new ranging system, based on National Instrument USRP 2954 board, is currently underway, aiming at assessing the BIRALET radar performances[24]. Targeted observations are performed, on December 13, 2019, by pointing the system towards 9 calibration objects from the International Laser Ranging Service (ILRS) database, which provides the positional state of the satellites with an accuracy of around a centimeter. The resulting measurements are compared against the associated accurate ephemerides. First, the observable passages of the objects are predicted, then the transmitter and the receiver are pointed accordingly, in order to observe them.
Also in this case, the BIRALET system was employed in a beam-parking mode, waiting for the objects to cross the FOV of the antenna, for a preliminary measurement campaign, in order to validate the integration of the new ranging system, described above in sub-section 3.3. A calibration measurement of the receiver chain was performed with the aim to investigate the received signal delay. In this way, we compensated the time error, and consequently the range error, caused by the receiver chain from the P-band receiver to the dedicated backend based on USRP 2954 board (see Figure 6). After this important calibration, a set of ILRS objects were detected on December 13, 2019, to compare the measured range rate (Doppler shift) and range, with the data available from the associated accurate ephemerides. In Table 4, the slant-range and range rate errors, obtained as the difference between the measured and the estimated values, are reported for the ILRS objects (SCNs 36508 and 41335, for which accurate ephemerides were available) and other targets (for which TLEs were adopted)[24].

SCN	Epoch	Slant-range error [m]	Range rate error [Hz]
16791	2019/12/13 9:07:54	-4	-3
36508	2019/12/13 9:53:25	67	-5
41335	2019/12/13 10:05:06	-69	-32
40697	2019/12/13 10:30:38	-35	-51

37387	2019/12/13 10:47:54	-84	-28
40894	2019/12/13 10:59:38	0	-38
5395	2019/12/13 11:15:16	75	10
11962	2019/12/13 11:26:58	-31	-3
38338	2019/12/13 11:54:33	40	11

Table 4: Preliminary results of the testing measurement campaign on December 13, 201924

The analysis of the data from Table 4, collected by the BIRALET radar, shows that we have a slant-range and Doppler shift error compatible with the requirements requested by the EUSST program[24]. However, the calibration measurement campaign must be repeated periodically in order to update these results and maintain the high performance of the system.

5. CONCLUSIONS AND FUTURE WORKS

The BIRALET system is a bi-static radar that collects useful data for space debris studies. The system is composed of the TRF antenna as transmitter, that permits, thanks to its back-end based on USRP 2954 board, to transmit a continuous or modulated signal, in order to perform range and range rate measurements. The receiver is the SRT antenna, which can be equipped with three dedicated acquisition chains, each one with a dedicated back-ends. The simplest channel is based on the use of the FSV model Spectrum Analyzer from Rohde and Schwartz. This configuration is useful for fast experiments where it is necessary to view the acquired spectra immediately and it permits to perform Doppler shift measurements with an accuracy less than 10 Hz. The second configuration consists of a receiving chain that shift the RF signal at 410 MHz to an intermediate frequency at 30 MHz in the range of the Red Pitaya board, used as back-end. This configuration remedies the limitations of the Spectrum Analyzer, i.e. the slow frequency sweeps for low resolution bandwidths, thus preventing all data saving in real time, and it guarantees a Doppler shift measurements with an accuracy lower than 20 Hz. The third back-end is based on a National Instrument USRP 2954 board, which allows range and range rate measurements with an accuracy of 30 meters and a few Hz.

The preliminary results confirm that the measurements collected by the BIRALET radar, after calibration and bias correction, are accurate and comply with the design and simulations. An improvement of the system can be done by increasing the integration time (increasing the number of integrated pulses of Figure 9) or changing the transmitted waveform. Many tests can be done by tuning the system parameters, and by processing the real time stored I/Q samples offline. Further measurements and processing refinements will be made in the next few months, in order to evaluate the performances of the system. The evaluation will be tested on coverage and accuracy, using several targets with different radar cross sections and orbiting altitudes.

One of the physical limitations of the current BIRALET system could be the relatively low mechanical tracking speed of the SRT (0.85 deg/sec in azimuth, 0.5 deg/sec in elevation, as listed in Table 1) and the availability of only one beam, resulting in a limited field of view (HPBW of 0.8 degrees, as reported in Table 1). Space debris, with angular speed greater than the maximum antenna angular movement, cannot be tracked[22]. In addition, it proves impossible to measure the object trajectory direction with only one beam, as is the case of the actual P-band BIRALET radar. Imaging the sky with a multi-beam receiver would increase the telescope field of view and survey speed, allowing the coverage of a greater portion of the sky in less time[22]. One way to do it, as a future project, would be to use a Phased Array Feed (PAF) as a receiver for the primary focus of SRT[22,25,28]. A PAF is made up of closely packed antenna elements that, by spatially sampling the focal plane, can synthesize multiple independent beams. Beam shapes and directions are controlled electronically by weighting the amplitudes and phases of the signals acquired by each individual antennas with a beam-former[26,27]. Consequently, through the beam-forming process, PAFs are able to synthesize multiple beams and optimize each of them, enhancing aperture efficiency as well as effective field-of-view. The beam shapes and side lobes can be modified in real time and be set to minimize their response, in relation to undesired radio frequency interferences.

REFERENCES

[1] Ruggiero, A., Pergola, P. and Andreucci, M., "Small Electric Propulsion Platform for Active Space Debris Removal," IEEE Transactions on Plasma Science 43(12), 4200-4209 (2015).

[2] Klinkrad, H., [Hypervelocity Impact Damage Assessment and Protection Techniques], Space Debris – Models and Risk Analysis, Ed. Springer, 199-205 (2006).

[3] Hoots, F. R., Schumacher, P. W. and Glover, R. A., "History of Analytical Orbit Modeling in the U.S. Space Surveillance System," Journal of Guidance Control and Dynamics 27(2), 174-185 (2004).

[4] Vallado, D. A. and Griesbach, J. D., "Simulating Space Surveillance Networks," Proc. AAS/AIAA Astrodynamics Specialist Conference, (2011).

[5] Klinkrad, H., [The Current Space Debris Environment and its Sources], Space Debris – Models and Risk Analysis, Ed. Springer, 5-18 (2006).

[6] Masekell, P. and Lorne, O., "Sapphire: Canada's Answer to Space-Based Surveillance of Orbital Objects," Proc. Advanced Maui Optical and Space Surveillance (AMOS) Conference, (2008).

[7] Markkanen, J., Lehtinen, M. and Landgraf, M., "Real-time space debris monitoring with EISCAT," Advances in Space Research 35(7), 1197-1209 (2005).

[8] Mehrholz, D., Leushacke, L. and Jehn, R., "The COBEAM-1/96 Experiment," Advances in Space Research 23(1), 23-32 (1999).

[9] Wilden H. et. al, "GESTRA – A Phased-Array Based Surveillance and Tracking Radar for Space Situational Awareness," Proc. IEEE International Symposium on Phased Array Systems and Technology (PAST), 1-5 (2016).

[10] Ender, J., Leushacke, L., Brenner, L. and Wilden, H., "Radar Techniques for Space Situational Awareness," Proc. IEEE Proceedings International Radar Symposium (IRS), 21-26 (2011).

[11] Klinkrad, H., "Monitoring Space – Efforts Made by European Countries," Proc. International Colloquium on Europe and Space Debris, (2002).

[12] Gomez I. A. et al., "Description of the Architecture of the Spanish Space Surveillance and Tracking System," Proc. 7th European Conference on Space Debris, (2017).

[13] Ladd D., et al., "Technical Description of a Novel Sensor Network Architecture and Results of Radar and Optical Sensors contributing to a UK Cueing Experiment," Proc. Advanced Maui Optical and Space Surveillance (AMOS) Conference, (2017).

[14] Pisanu, T., Schirru, L., Urru, E., Gaudiomonte, F., Ortu, P., Bianchi, G., Bortolotti, C., Roma, M., Muntoni, G., Montisci, G., Protopapa, F., Podda, A., Sulis, A. and Valente, G., "Upgrading the Italian BIRALES System to a Pulse Compression Radar for Space Debris Range Measurements," Proc. IEEE 22nd International Microwave and Radar Conference (MIKON), 317-320 (2018). doi: 10.23919/MIKON.2018.8405212.

[15] Muntoni, G. et al., "A Space Debris-Dedicated Channel for the P-Band Receiver of the Sardinia Radio Telescope: A Detailed Description and Characterization," IEEE Antennas and Propagation Magazine 62(3), 45-57 (2020). doi: 10.1109/MAP.2019.2943274.

[16] Losacco, M., Di Lizia, P., Massari, M., Mattana, A., Perini, F., Schiaffino, M., Bortolotti, C., Roma, M., Naldi, G., Pupillo, G., Bianchi, G., Lama, L., Cutajar, D., Magro, A., Portelli, C., Reali, M, Villadei, W., "The multibeam radar sensor BIRALES: performance assessment for space surveillance and tracking," Proc. 69th International Astronautical Congress (IAC), (2018).

[17] Muntoni, G., Schirru, L., Pisanu, T., Montisci, G., Valente, G., Gaudiomonte, F., Serra, G., Urru, E., Ortu P. and Fanti A., "Space debris detection in Low Earth Orbit with the Sardinia Radio Telescope," Electronics 6(3), 1-16 (2017). doi: 10.3390/electronics6030059.

[18] Losacco, M. and Schirru, L., "Orbit Determination of Resident Space Objects Using the P-Band Mono-Beam Receiver of the Sardinia Radio Telescope,", Applied Sciences 9(19), 4092 (2019). doi: 10.3390/app9194092

[19] Bolli, P., et al., "A novel application of the active surface of the shaped Sardinia radio telescope for primary-focus operations," IEEE Antennas Wireless Propag. Lett., 13, 1713–1716 (2014).

[20] R&S®FSV Signal and Spectrum Analyzer, https://www.rohde-schwarz.com/us/product/fsv-productstartpage_63493-10098.html?change_c=true

[21] Red Pitaya board, https://www.redpitaya.com/

[22] Schirru, L. et al., "Advantages of Using a C-band Phased Array Feed as a Receiver in the Sardinia Radio Telescope for Space Debris Monitoring," Proc. 2019 IEEE 2nd Ukraine Conference on Electrical and Computer Engineering (UKRCON), 133-136 (2019). doi: 10.1109/UKRCON.2019.8879919.

[23] National Instrument, Specifications USRP-2954, www.ni.com/pdf/manuals/375725c.pdf
[24] Pisanu, T., Schirru, L., Urru, E., Bianchi, G., Podda, A., Di Lizia, P., "The Italian Biralet Radar System To Perform Range And Range Rate Measurements In The Eusst European Space Surveillance And Tracking Program," Proc. 71th International Astronautical Congress (IAC), (2020).
[25] Pisanu, T., Schirru, L., Urru, E., Navarrini, A., Muntoni, G., Melis, A., Concu R. and Ortu, P., "Design and simulations of a phased array feed for the biralet radar," Proc. 70th International Astronautical Congress (IAC), (2019).
[26] Navarrini, A. et al., "The Warm Receiver Section and the Digital Backend of the PHAROS2 Phased Array Feed," Proc. 2019 IEEE International Symposium on Phased Array System & Technology (PAST), 1-8 (2019). doi: 10.1109/PAST43306.2019.9021018.
[27] Navarrini, A., Scalambra, A., Rusticelli, S., Maccaferri, A., Cattani, A., Perini, F., Ortu, P., Roda, J., Marongiu, P., Saba, A., Poloni, M., Ladu, A. and Schirru, L., "The Room Temperature Multi-Channel Heterodyne Receiver Section of the PHAROS2 Phased Array Feed," Electronics 8(6), 666 (2019). doi: 10.3390/electronics8060666.
[28] Navarrini, A., Nesti, R. and Schirru, L., "Electromagnetic simulation and beam-pattern optimization of a C-band Phased Array Feed for the Sardinia Radio Telescope," Proc 2019 IEEE 2nd Ukraine Conference on Electrical and Computer Engineering (UKRCON), 137-143 (2019). doi: 10.1109/UKRCON.2019.8879888.